Published in final edited form as:
Free Radic Biol Med. 2007 October 1; 43(7): 1076–1085. doi:10.1016/j.freeradbiomed.2007.06.022.

Interactions of the Major Metabolite of the Cancer Chemopreventive Drug Oltipraz with Cytochrome C: A Novel Pathway for Cancer Chemoprevention

Murugesan Velayutham[a,*], **Rajendra B. Muthukumaran**[b], **Joe Z. Sostaric**[a], **John McCraken**[b], **James C. Fishbein**[c], and **Jay L. Zweier**[a,*]

[a] Center for Biomedical EPR Spectroscopy and Imaging, the Davis Heart and Lung Research Institute, and the Division of Cardiovascular Medicine, the Department of Internal Medicine, The Ohio State University College of Medicine, Columbus, Ohio 43210

[b] Department of Chemistry, Michigan State University, East Lansing, Michigan 48824

[c] Department of Chemistry and Biochemistry, University of Maryland Baltimore County, 1000 Hilltop Circle, Baltimore, Maryland 21250

Abstract

The major metabolite of the cancer chemopreventive agent oltipraz (OLT), a pyrrolopyrazine thione (PPD), has been shown to be a phase two enzyme inducer, an activity thought to be key to the cancer chemopreventive action of the parent compound. In cells, mitochondria are the major source of reactive oxygen species (ROS) and cytochrome c (cyt c) is known to participate in mitochondrial electron transport and confer antioxidant and peroxidase activities. To understand possible mechanisms by which PPD acts as a phase two enzyme inducer, a study of its interaction with cyt c was undertaken. UV-visible spectroscopic results demonstrate that PPD is capable of reducing oxidized cyt c. The reduced cyt c is stable for a long period of time in the absence of an oxidizing agent. In the presence of ferricyanide, the reduced cyt c is rapidly oxidized back to its oxidized form. Further, UV-visible spectroscopic studies show that during the reduction process the co-ordination environment and redox state of iron in cyt c is changed. Low temperature EPR studies show that during the reduction process, the heme iron changes from a low spin state of s = ½ to a low spin state of s = 0. Room temperature EPR studies demonstrate that PPD inhibits the peroxidase activity of cyt c. EPR spin trapping experiments using DMPO show that PPD inhibits the superoxide radical scavenging activity of oxidized cyt c. From these results, we propose that PPD interacts with cyt c, binding to and then reducing the heme, and this may enhance ROS levels in mitochondria. This in turn could contribute to the mechanism by which the parent compound, oltipraz, might trigger the cancer chemopreventive increase in transcription of phase 2 enzymes.

Address correspondence to: Jay L. Zweier, MD, Director, Davis Heart and Lung Research Institute, 473 W. 12th Ave, Room 110G, The Ohio State University, Columbus, OH 43210, Phone: 614–247–7857, Fax: 614–247–7845, E-mail: Jay.Zweier@osumc.edu and Murugesan Velayutham, Ph.D, TMRF, Room 130, 420, W. 12th Avenue, The Ohio State University, Columbus, OH - 43210, Phone: 614–292–9082, Fax: 614–292–8454, E-mail: Velayutham.1@osu.edu.

The modifications of cyt c function by the oltipraz metabolite may have implications for the regulation of apoptotic cell death.

Keywords

EPR; Oltipraz; DTMO; PPD; metabolite; cytochrome c; chemoprevention; cancer; reactive oxygen species; ROS; dithiolethiones; phase 2 enzymes; Free radical

Introduction

Many dietary and synthetic compounds have been found to potently inhibit carcinogenesis. We are currently engaged in trying to understand the molecular basis for the cancer chemopreventive action of dithiolethiones (1,2-dithiole-3-thiones). Oltipraz (OLT) is a member of the class of compounds called dithiolethiones and has been in Phase 2 clinical trials for the prevention of aflatoxin-induced hepatocellular carcinoma [1–4]. Dithiolethiones are believed to afford protection from electrophilic and oxidative assault because they raise the levels of many phase 2 enzymes. These enzymes are traps of electrophiles and reactive oxygen species and are also conjugating enzymes that prepare metabolites for export [5–7]. Oltipraz also acts as a chemopreventive agent against colorectal and urinary bladder cancers in rat models [8–11].

Oltipraz was originally used as an antischistosomal agent, and the metabolism of oltipraz by humans has been studied [12]. During metabolism, approximately 1% of the original compound is converted to an oxo analog (3OO, Scheme 1), which is itself a phase 2 enzyme inducer [13,14]. The major isolated metabolite is a dimethylated pyrrolopyrazine, (MPP, Scheme 1). It was recently shown that MPP is produced by the biological methylation of the intermediate pyrrolopyrazine-thione (PPD, Scheme 1), an anion at physiological pH (conjugate acid pKa = 4.32) [15]. The reaction kinetics of DTMO (Scheme 1) with GSH to form PPD was well characterized and the rate constant is $6.65 \times 10^6\ M^{-1}\ s^{-1}$ [15]. It has also been demonstrated that PPD is a phase 2 enzyme inducer with a potency on par with oltipraz itself [16].

The biochemical basis for cancer chemoprevention by dithiolethiones including oltipraz is becoming increasingly clear [5,13,17–23]. The induction of phase 2 enzymes by dithiolethiones is mediated by a 41 base pair enhancer element known as the anti-oxidant response element (ARE) that is found upstream of the coding regions of many phase 2 genes. Activation mediated by the ARE is effected by transcription factor Nrf2, which is essential for the chemopreventive efficacy of oltipraz and its metabolites [16,24,25]. Nrf2 is largely sequestered in the cytosol, bound to the chaperone Keap1, a cysteine rich protein, which is anchored to the cytoskeleton by binding to actin. Thiol reactive agents, including dithiolethiones, have been shown to un-tether Nrf2 and permit/induce its translocation to the nucleus [22,26].

Two general hypotheses have been advanced concerning the mechanisms of activation of Nrf2. The first notion suggests that oltipraz, or perhaps a product of its reaction with cellular thiols acts as an electrophile, binding to a protein thiol and may subsequently effect the

closure of a dithiol linkage in Keap1 [19,27,28]. The second suggestion was that oltipraz and other dithiolethiones induce transcription by initiating a flux of “reactive oxygen species” (ROS) [29]. This was based on the observation that oltipraz, and other dithiolethiones, induce nicking of supercoiled DNA in a reaction that was dependant upon the presence of thiols, oxygen and metal ions, but which could be inhibited by catalase. Presumably peroxides activated a redox sensitive transcription factor, for which there is precedent [26], or possibly altered the structure of thiol-rich Keap1, thus effecting the release of Nrf2. Our recent studies showed that oltipraz itself and PPD in the presence of GSH generate ROS [30,31].

It has been shown that oltipraz stimulates transcription of the mitochondrial superoxide dismutase (manganese SOD; Mn-SOD) gene through the increase of ROS [32] and it has also been shown to inhibit apoptosis [33]. In mammalian cells, the mitochondria are a major source of reactive oxygen species [34]. Furthermore, cytochrome c (cyt c) is a small, globular heme protein which exists in high concentration (0.4 mM) [35] in the inner membrane of mitochondria. At least 15 % of cyt c is tightly bound to the inner membrane and the remainder is loosely attached to the inner membrane and can be readily mobilized [36]. Physiologically, cyt c mediates electron shuttling between cytochrome c reductase (complex III) and cytochrome c oxidase (complex IV) during mitochondrial respiration [36]. The loosely associated cyt c participates in electron transport, mediates superoxide removal and prevents oxidative stress [36–38] while the tightly bound cyt c accounts for the peroxidase activity [39]. Release of cytochrome c (cyt c) from the inner mitochondrial membrane into the cytosol is a proapoptotic factor [40,41]. Therefore, we are interested in the molecular details of the interaction of the major metabolite of oltipraz with cyt c and of the potential contribution of this interaction to chemoprotection.

In this study, we have employed the sensitive and specific techniques of electron paramagnetic resonance (EPR) and UV-visible absorption spectroscopy to study the interaction of the metabolite of oltipraz (PPD) with cyt c and its effect on cyt c’s antioxidant activity.

Materials and methods

Materials

7-methyl-6,8-bis(methyldisulfanyl)pyrrolo[1,2-a]pyrazine (DTMO) was synthesized as reported [15]. All other chemicals were obtained from commercial sources and were of analytical grade. Oxidized cytochrome c (Fe^{III}cyt c, from horse heart), xanthine oxidase (Grade III from buttermilk), xanthine sodium salt, reduced glutathione (GSH), hydrogen peroxide (H_2O_2), and potassium ferricyanide ($K_3Fe(CN)_6$) were purchased from Sigma. Diethylenetriaminepentaacetic acid (DTPA) and sodium L-ascorbate were obtained from Aldrich. Purified 5,5-Dimethyl-1-pyrroline-*N*-oxide (DMPO) was purchased from Dojindo laboratories, Kumamoto, Japan.

UV-visible spectrophotometry

Optical spectra were measured on a Cary 50 Bio UV-visible spectrophotometer. All experiments were carried out in phosphate buffer solution, pH 7.4, containing 0.1 mM DTPA.

EPR measurements

Solution EPR spectra were recorded using quartz flat cells at room temperature with a Bruker ESP 300E spectrometer operating at X-band with 100 kHz modulation frequency and a TM_{110} cavity. Room temperature EPR spectra were recorded using the parameters described in the Fig. legends. All the experiments were carried out in phosphate buffer solution, pH 7.4, containing 0.1 mM DTPA.

Low temperature (12 K) EPR Spectra were obtained at X-band using a Bruker ER300E spectrometer equipped with a TE_{102} ESR cavity and an Oxford ESR-900 cryostat. The external magnetic field strength was measured with a Bruker ER 035M NMR Gaussmeter and the microwave frequency was determined with an EIP 25B frequency counter. The samples were placed in quartz tubes and frozen at 77 K. The frozen samples were placed inside the cavity and continuous wave EPR spectra were taken with the following spectrometer conditions: modulation frequency 100 kHz; modulation amplitude 8 G; time constant 10 ms; sweep time 84 s; microwave power 2 mW; sample temperature 12 K; number of scans 5.

Mass spectrometry

The product formed during the reaction between PPD and cyt c was analysed on a Micromass LCT electrospray mass spectrometer. The mass spectrometer conditions were electrospray positive ion mode with the source temperature 100 °C, desolvation temperature at 100 °C, capillary voltage 3000 V, cone voltage 55 V, cone gas flow at ca. 100 L/h, and the desolvation gas flow at ca. 500 L/h.

Results

UV-visible absorption studies of PPD

The alternate precursor DTMO reacts to completion with GSH in a 1:2 molar ratio to form the metabolite PPD and GSSG [15]. The metabolite, PPD, in aqueous buffer medium was yellow in color and the UV-visible absorption spectrum is shown in Fig. 1. The spectrum showed three absorption bands at 313, 373, and 449 nm. No absorption band was observed above 500 nm.

UV-visible absorption studies of PPD and cyt c

The heme group of cyt c contains iron, which can change from the oxidized state (Fe^{III}) to the reduced state (Fe^{II}) in the presence of reducing agents [42,43]. In addition to this, exogenous ligands interact with the heme group of cyt c and change the co-ordination of iron [44]. UV-visible spectrophotometry was used to explore the effect of PPD on cyt c; as shown in Fig. 2.

The UV-visible absorbance spectrum of a phosphate buffered solution of ferricytochrome c (Fe^{III}cyt c; 50 μM) is shown in Fig. 2 in the wavelength range of 450 to 650 nm (Fig. 2A) and on an expanded absorbance scale in the wavelength range of 600 to 800 nm (Fig. 2B). Also shown in Fig. 2 is the effect of PPD on the spectrum of Fe^{III}cyt c and the effect of subsequent addition of potassium ferricyanide to the Fe^{III}cyt c and PPD solution. The spectrum of Fe^{III}cyt c (50 μM) solution did not change with time and consists of the expected broad, unresolved absorption band with a maximum at 528 nm (Fig. 2A(I)) and a weak absorption band at 695 nm (Fig. 2B(I)). The addition of PPD (50 μM) to the Fe^{III}cyt c (50 μM) solution resulted in two new peaks at 520 nm and 550 nm (Fig. 2A(II)). These peaks correlate with the absorbance characteristics of Fe^{II}cyt c solution [43], indicating that PPD has reduced Fe^{III}cyt c to Fe^{II}cyt c. No change in the absorbance was observed at 550 nm after two hours, indicating that Fe^{II}cyt c was stable. Furthermore, the loss of the absorption band at 695 nm on the addition of PPD to Fe^{III}cyt c (Fig 2B(II)) is a clear indication that there is a change in the co-ordination of iron [43].

To confirm that PPD reduced Fe^{III}cyt c to Fe^{II}cyt c we studied the effect of potassium ferricyanide on the Fe^{III}cyt c and PPD solution, since it is known that ferricyanide rapidly oxidizes Fe^{II}cyt c to Fe^{III} cyt c [45]. When ferricyanide (0.1 mM) was added to the Fe^{III}cyt c solution containing PPD, the resulting spectrum (Fig. 2A(III) and Fig. 2B(III)) was almost identical to that of the original phosphate buffered Fe^{III}cyt c solution (Fig. 2A(I) and 2B(I)). This result shows that PPD-reduced cyt c can be re-oxidized by strong oxidizing agents.

EPR spectroscopy of PPD and cyt c

It has been demonstrated that exogenous ligands interact with the heme group of cyt c and change the co-ordination and redox states of iron [44]. EPR spectroscopy has been extensively utilized to monitor the redox state and co-ordination of iron in cyt c [45–47]. Low-temperature (12 K) EPR measurements were performed to support the spectrophotometric experiments on the reaction of PPD with cyt c. The EPR spectrum of a frozen solution of the Fe^{III}cyt c is shown in Fig. 3A and that of a frozen solution containing PPD and Fe^{III}cyt c is shown in Fig. 3B. For the latter solution, the EPR spectral features due to the Fe^{III}cyt c were eliminated, and a very distinctive spectrum appeared (Fig. 3B). The intensity of this EPR spectrum was less than 10 %, of the intensity of the free Fe^{III}cyt c spectrum (Fig. 3A). This shows that more than 90 % of Fe^{III}cyt c was reduced by PPD. It is known that potassium ferricyanide takes up a reducing equivalent from Fe^{II}cyt c, and when added to a Fe^{II}cyt c solution, resulted in the regeneration of Fe^{III}cyt c [45]. This behavior was reflected by the EPR spectrum measured after the addition of excess potassium ferricyanide to a solution containing Fe^{III}cyt c, and PPD (Fig. 3C). This result demonstrates that PPD changes the oxidation state and co-ordination of iron in cyt c.

Characterization of the reaction product of PPD and cyt c

In order to identify and characterize the reaction product of PPD and cyt c, mass spectroscopic studies were carried out. The mass spectrum of the reaction mixture containing PPD and cyt c showed a protonated molecular ion peak at 390.8 m/z (Fig. 4), which is consistent with the dimerization of PPD. This study demonstrated that the oxidation

of PPD produces a dimerized product of PPD and that the mechanism appears to occur via the production of an unstable radical intermediate of PPD.

Effect of PPD on antioxidant activity of cyt c

It has been suggested that cyt c can function as an antioxidant oxidizing the superoxide radical into molecular oxygen under physiological conditions [37,38,42]. Therefore, we wanted to study the effect of PPD on the possible antioxidant function of cyt c. EPR spin trapping experiments were carried out to investigate the effect of PPD on the superoxide radical scavenging activity of Fe^{III}cyt c. Superoxide radicals were enzymaticaly generated using xanthine oxidase (XO) and xanthine. The EPR spectrum was recorded for the phosphate buffered solution (pH 7.4) containing XO (0.02 U/mL), xanthine (333 μM), and DMPO (50 mM). The observed EPR spectrum was due to the superoxide radical adduct of DMPO (DMPO-OOH), as shown in Fig. 5A. From the spectrum, the calculated isotropic hyperfine values are a_N = 14.2 G, a_{H1} = 11.6 G, and a_{H2} = 1.2 G, which is in agreement with reported values [30]. Addition of Fe^{III}cyt c (0.1 mM) to the phosphate buffered solution containing XO (0.02 U/mL), xanthine (333 μM), and DMPO (50 mM) quenched the EPR signal (Fig. 5B). Cyt c converts the superoxide radical into molecular oxygen [37]. The addition of PPD (0.1 mM) and Fe^{III}cyt c (0.1 mM) to the phosphate buffered solution containing XO (0.02 U/mL), xanthine (333 μM), and DMPO (50 mM) produced the EPR spectrum of DMPO-OOH, as shown in Fig. 5C. (Note that the PPD reacts in a 1:1 molar ratio (and to completion) with oxidized cyt c to form reduced cyt c and a dimer of PPD. In Fig. 5C there is no excess PPD remaining to influence the formation of DMPO-OOH adducts by the X/XO system). These results show that PPD inhibits the superoxide radical scavenging function of cyt c.

Effect of PPD on peroxidase activity of cyt c

It has been demonstrated that cyt c acts as a peroxidase and is involved in the detoxification of hydrogen peroxide (H_2O_2) [39,48]. During peroxidatic activity FeIIIcyt c reacts with H_2O_2 to form the peroxidase compound I-type intermediate, as shown in Scheme 2. The peroxidase compound I-type intermediate enhanced the oxidation of ascorbate into its radical form, which has been characterized using the EPR spectroscopic technique [49].

EPR experiments were performed in order to study the effect of PPD on the peroxidase activity of cyt c. The EPR spectrum of ascorbate alone in phosphate buffer contained a background signal as shown in Fig. 6A. The background signal was due to the autooxidation of ascorbate into the ascorbate radical [50]. No change in the EPR spectrum was observed by the addition of either H_2O_2 (0.25 mM) or Fe^{III}cyt c (25 μM) (Figs. 6B&C). The EPR spectrum recorded for the solution containing ascorbate (1 mM), Fe^{III}cyt c (25 μM), and H_2O_2 (0.25 mM) produced a relatively intense signal, as shown in Fig. 6D. However, the addition of PPD (25 μM) to the reaction mixture resulted in a decrease of signal intensity (Fig. 6G). (Note that the concentration of H_2O_2 used is 10 times higher than the PPD concentration, therefore the effect described above can not be due to direct reaction between PPD and H_2O_2). The oxidation of ascorbate was not increased by the PPD alone or in the absence of cyt c or H_2O_2 (Figs. 6E&F). Thus, PPD binds to and reduces cyt c inhibiting the formation of the compound-I type intermediate.

Discussion

In the current study, the metabolite PPD was formed instantaneously and quantitatively from the alternative precursor DTMO in the presence of GSH. UV-visible absorption studies suggest that PPD acts as a strong reducing agent and reduces Fe^{III}cyt c to Fe^{II}cyt c. The increase of PPD concentration had no effect on the absorption value at 550 nm and it showed that PPD could not oxidize Fe^{II}cyt c. Furthermore, PPD by binding to and reducing Fe^{III}cyt c inhibited the peroxidase and antioxidant activities of cyt c.

In Fe^{III}cyt c, the sulfur atom of methionine (Met-80) occupies the sixth coordination site of the heme iron and it is relatively labile [45]. The methionine sulfur coordination can be easily displaced by exogenous ligands [44]. Earlier work has shown that Met-80 plays a crucial role in the mechanism of reduction of heme iron by exogenous ligands [45]. The absorption band at 695 nm is characteristic of the binding of the Met-80 sulfur with the heme iron in the sixth coordination site [51]. The reaction of Fe^{III}cyt c with PPD led to changes in spectral properties, most notably the disappearance of the absorption band at 695 nm, indicating that Met-80 ceases to coordinate with the heme iron. This could be due to the binding of PPD with the heme iron followed by reduction of the iron to Fe^{II}, as shown in Scheme 3.

The coordination of PPD with the heme iron in Fe^{II}cyt could be labile. However, no change in the absorption value at 550 nm for Fe^{II}cyt c was observed even after two hours of measurement. This showed that Fe^{II}cyt c was stable and that the sulfur atom of Met-80 could not replace the bonded PPD from the iron center. It also showed that there was no autooxidation of Fe^{II}cyt c.

It has been shown that ferricyanide can rapidly oxidize ferrocytochrome c into ferricytochrome c [45]. The rapid oxidation of reduced cytochrome c by ferricyanide, at neutral pH, resulted in the appearance of the absorbance maximum at 695 nm and decay of the peak at 550 nm (Figs. 2A&B). No change was observed in the UV-visible spectra of "regenerated" Fe^{III}cyt c compared to the UV-visible spectra of Fe^{III}cyt c alone, (Figs. 2A&B). From these studies it was clear that PPD can reduce Fe^{III}cyt c, however, in the presence of strong oxidizing agents, Fe^{II}cyt c can be re-oxidized to its original state, as shown in Scheme 3. In the presence of ferricyanide the sulfur atom of Met-80 bonded with the heme iron at the sixth coordination position. These results show that in cyt c the axial coordination of PPD with heme iron is stronger than the Met-80 coordination, as might be expected.

In order to confirm the change in redox state of the iron in cyt c, low-temperature (12K) EPR measurements were performed. EPR techniques are the best tool to address the changes in the oxidation state and spin multiplicity of the metal center in cyt c [46]. The low-temperature EPR spectrum of the Fe^{III}cyt c frozen solution showed a rhombic EPR signal (Fig. 3A), but with only two resolved g-values, characteristic of low-spin ferric six-coordinated heme iron. The observed g-values were $g_1 = 3.071$, and $g_2 = 2.234$, which are in agreement with the literature [47]. The third g-value could be calculated ($g_3 = 1.257$) from these two g-values assuming $\Sigma g^2 = 16$ [52]. With the addition of the metabolite PPD, the

characteristic peaks due to the free Fe^{III}cyt c were eliminated and a very distinctive rhombic EPR feature was observed (Fig. 3B). The feature is presumed to be indicative of the distortions in the inner coordination sphere of Fe^{III}cyt c [46]. However, the intensity of this EPR spectrum was less than 10 %, compared with that of the spectrum of free Fe^{III}cyt c. The observed g-values of this new species were $g_1 = 2.539$, $g_2 = 2.308$, and $g_3 = 1.87$. The observed g-values were markedly different from the free Fe^{III}cyt c and may be attributed to the displacement of methionine possibly by PPD binding. The low temperature EPR spectrum recorded for the solution containing Fe^{III}cyt c and PPD in the presence of excess potassium ferricyanide showed a rhombic EPR spectrum similar to the free Fe^{III}cyt c. In addition, a very weak EPR feature due to PPD and Fe^{III}cyt c (Fig. 3B) was also observed (Fig. 3C, labeled *). These EPR results confirmed that most of the Fe^{III}cyt c had been reduced by the addition of the metabolite, PPD. EPR studies also demonstrated that during the reduction process, low spin Fe^{III}cyt c (s = 1/2) is converted into Fe^{II}cyt c. These findings are consistent with the optical studies that PPD reduces Fe^{III}cyt c to Fe^{II}cyt c. In order to characterize the reaction product of PPD and cyt c, mass spectroscopic studies were carried out (Fig. 4) where it was confirmed that the product of PPD oxidation was a dimer of PPD. This suggests that the product was formed through a radical intermediate.

The cytochrome c assay, which involves the reduction of ferricytochrome c by the superoxide radical, is one of the most frequently used assays for the detection of superoxide radical in biological chemistry. However, if the agent being tested reduces Fe^{III}cyt c instantaneously, the assay would not be useful for the detection of superoxide radicals [53]. Under these circumstances EPR spin trapping experiments are more specific and sensitive for the detection of the superoxide radical [54]. DMPO traps the superoxide radical generated by the XO and xanthine system to form the DMPO-OOH adduct (Fig. 5A). The signal from the DMPO-OOH adduct is quenched by the addition of cyt c to the solution, as shown in Fig. 5B. However, in the presence of PPD, the superoxide radical generated by XO and xanthine could not be scavenged by cyt c and the EPR spectrum of DMPO-OOH adducts is shown in Fig. 5C. In accordance with the spectrophotometric studies, PPD reduces the heme-iron and blocks the incoming superoxide radical. It has already been shown that superoxide radical does not react with ferrocytochrome c [42]. These results demonstrate that PPD inhibited the superoxide radical scavenging activity of ferricytochrome c.

Recently Lawrence et al. have shown that the Fe^{III}cyt c/H_2O_2 couple could form a peroxidase compound I-type intermediate and oxidize cellular antioxidants such as GSH, NADH, and ascorbate to their respective radicals [49]. The enhanced oxidation of ascorbate into ascorbate radical by peroxidase compound I-type intermediate (Scheme 2) was studied using the EPR spectroscopic technique [49]. We extended our studies to examine the effect of PPD on the peroxidase function of Fe^{III}cyt c. Auto-oxidation of ascorbate gave ascorbate radical, which was stable and gave a characteristic doublet spectrum in the EPR spectrum with the hyperfine value of 1.7 G [49]. In the presence of the Fe^{III}cyt c/H_2O_2 couple the EPR signal intensity of the ascorbate radical was enhanced to a greater extent, (Fig. 6D). However, the addition of PPD did not increase the oxidation of ascorbate, (Fig. 6G). This showed that the addition of PPD inhibited the oxidation of ascorbate into the ascorbate

radical. These results showed that PPD binds with the heme-iron and blocks the incoming H_2O_2 from forming the peroxidase compound I-type intermediate.

The EPR spin trapping results (Fig. 5) demonstrate that PPD inhibits the antioxidant activity of cyt c. In mitochondria, the electron transport chain complexes I and III are the main sites of superoxide radical production [34,55,56]. The loosely bound cyt c at the membrane acts as an antioxidant and catalyzes the conversion of the superoxide radical into molecular oxygen [37]. Therefore, the inhibition of the antioxidant function of cyt c by PPD could result in an increased amount of both superoxide radical anion and oxidative stress in mitochondria as the self dismutation of superoxide radicals leads to the formation of hydrogen peroxide [57]. However, the membrane bound cyt c acts as a peroxidase and is involved in the detoxification of hydrogen peroxide [39].

The EPR spectroscopic study (Fig. 6) shows that the metabolite of oltipraz inhibits the peroxidase function of cyt c. Therefore, the major metabolite of oltipraz may increase both the hydrogen peroxide level and oxidative stress in the mitochondria by inhibiting the antioxidant and peroxidase functions of cyt c. It is well known that hydrogen peroxide functions as a signaling agent, particularly in higher organisms [58,59]. Hydrogen peroxide readily modifies cysteine thiols and can accomplish the closure of a prospective dithiol sensor analogous to what appears to function in the prokaryotic OxyR redox switch [58,60]. The modifications of cysteine thiols in Keap1 are sufficient to dissociate Keap1/Nrf2 complex [27]. An earlier study showed Keap1 is a sensor of oxidative stress [61]. It has recently been suggested that Nrf2 is phosphorylated, by protein kinase C (PKC), PI3 kinase, and MAP kinases, following oxidative insult and that this modification disrupts Keap1/Nrf2 binding [62–66]. It is possible that the increased level of reactive oxygen species in mitochondria could initiate a mitochondrion to nucleus signaling pathway in which H_2O_2 or H_2O_2 and protein kinases dissociate Nrf2 from Keap1. Inhibition of the peroxidase activity of cyt c might enhance ROS flux and thereby augment phase 2 enzyme induction by the major metabolite of oltipraz as shown in Fig. 7.

The results discussed above show that the major metabolite of oltipraz inhibits the antioxidant and peroxidase functions of cyt c and could increase the reactive oxygen species in mitochondria. It has been demonstrated that oltipraz rapidly activates NF-κB in rat hepatocytes in primary culture, which may contribute to the early activation of mitochondrial SOD (Mn-SOD) gene transcription [32]. It has also been demonstrated that mitochondrial production of hydrogen peroxide activates protein kinase D, which in turn is required for Mn-SOD expression [67]. Based on our studies and the reported literature, we propose that the production of reactive oxygen species at the mitochondria could initiate a mitochondrion to nucleus signaling pathway as depicted in Fig. 7.

On a further point of discussion, it has been demonstrated that oltipraz inhibited apoptosis in the respiratory tract of rats exposed to cigarette smoke [33]. It is interesting to note that conformational change in cyt c is an early event in apoptosis [68]. In addition, the cyt c, after release from the mitochondria into the cytosol, binds with apoptotic protease activating factor-1 (Apaf-1), which oligomerizes and then activates pro-caspase-9 [69]. The UV-visible and EPR studies show that the metabolite of oltipraz binds with cyt c changing the active

site coordination. Therefore, the binding of the metabolite of oltipraz, PPD, with cyt c may be involved in the inhibition of the initial conformational change of cyt c. Alternatively PPD may be involved in the formation of apoptosomes with Apaf-1 which are required for apoptosis to occur.

In conclusion, UV-visible absorption and EPR studies show that the major metabolite of oltipraz is capable of reducing ferricytochrome c into ferrocytochrome c. EPR spectroscopic and spin trapping studies show that the metabolite PPD inhibits the peroxidase and antioxidant functions of cyt c respectively. These studies show that loss of the antioxidant capacity of cyt c may play a role in the cancer chemoprevention activity of oltipraz. The biological relevance of these findings remains to be elucidated and the correlation between cytochrome c and phase 2 enzyme induction requires further investigation.

Acknowledgments

This work was supported by National Institutes of Health Grants HL63744, HL65608, and HL38324 (JLZ) and GM54065 (JM). We thank Dr. R. P. Pandian for helpful discussion.

Abbreviations

$AscH^-$	ascorbate
DTPA	diethyltriaminepentaacetic acid
DMPO	5,5-dimethyl-1-pyrroline-*N*-oxide
EPR	electron paramagnetic resonance
GSSG	glutathione oxidized
GSH	glutathione reduced
H_2O_2	hydrogen peroxide
DTMO	7-methyl-6,8-bis(methyldisulfanyl)pyrrolo[1,2-a]pyrazine
OLT	oltipraz
Fe^{III}cyt c	oxidized cytochrome c
$K_3Fe(CN)_6$	potassium ferricyanide
PPD	pyrrolopyrazine-thione
Fe^{II}cyt c	reduced cytochrome c

References

1. Camoirano A, Bagnasco M, Bennicelli C, Cartiglia C, Wang JB, Zhang BC, Zhu YR, Qian GS, Egner PA, Jacobson LP, Kensler TW, De Flora S. Oltipraz chemoprevention trial in Qidong, People's Republic of China: results of urine genotoxicity assays as related to smoking habits. Cancer Epidemiol Biomarkers Prev. 2001; 10:775–783. [PubMed: 11440963]
2. Kensler TW, He X, Otieno M, Egner PA, Jacobson LP, Chen B, Wang JS, Zhu YR, Zhang BC, Wang JB, Wu Y, Zhang QN, Qian GS, Kuang SY, Fang X, Li YF, Yu LY, Prochaska HJ, Davidson NE, Gordon GB, Gorman MB, Zarba A, Enger C, Munoz A, Helzlsouer KJ, et al. Oltipraz chemoprevention trial in Qidong, People's Republic of China: modulation of serum aflatoxin

albumin adduct biomarkers. Cancer Epidemiol Biomarkers Prev. 1998; 7:127–134. [PubMed: 9488587]

3. Jacobson LP, Zhang BC, Zhu YR, Wang JB, Wu Y, Zhang QN, Yu LY, Qian GS, Kuang SY, Li YF, Fang X, Zarba A, Chen B, Enger C, Davidson NE, Gorman MB, Gordon GB, Prochaska HJ, Egner PA, Groopman JD, Munoz A, Helzlsouer KJ, Kensler TW. Oltipraz chemoprevention trial in Qidong, People's Republic of China: study design and clinical outcomes. Cancer Epidemiol Biomarkers Prev. 1997; 6:257–265. [PubMed: 9107431]
4. Glintborg B, Weimann A, Kensler TW, Poulsen HE. Oltipraz chemoprevention trial in Qidong, People's Republic of China: Unaltered oxidative biomarkers. Free Radic Biol Med. 2006; 41:1010–1014. [PubMed: 16934685]
5. Greenwald P. Cancer chemoprevention. Br Med J. 2002; 324:714–718. [PubMed: 11909790]
6. Hayes JD, McMahon M. Molecular basis for the contribution of the antioxidant responsive element to cancer chemoprevention. Cancer Lett. 2001; 174:103–113. [PubMed: 11689285]
7. Kensler TW. Chemoprevention by inducers of carcinogen detoxication enzymes. Environ Health Perspect. 1997; 105(Suppl 4):965–970. [PubMed: 9255588]
8. Rao CV, Tokomo K, Kelloff G, Reddy BS. Inhibition by dietary oltipraz of experimental intestinal carcinogenesis induced by azoxymethane in male F344 rats. Carcinogenesis. 1991; 12:1051–1055. [PubMed: 2044183]
9. Rao CV, Nayini J, Reddy BS. Effect of oltipraz [5-(2-pyrazinyl)-4-methyl-1,2-dithiol-3-thione] on azoxymethane-induced biochemical changes related to early colon carcinogenesis in male F344 rats. Proc Soc Exp Biol Med. 1991; 197:77–84. [PubMed: 2020672]
10. Rao CV, Rivenson A, Katiwalla M, Kelloff GJ, Reddy BS. Chemopreventive effect of oltipraz during different stages of experimental colon carcinogenesis induced by azoxymethane in male F344 rats. Cancer Res. 1993; 53:2502–2506. [PubMed: 8495412]
11. Iida K, Itoh K, Kumagai Y, Oyasu R, Hattori K, Kawai K, Shimazui T, Akaza H, Yamamoto M. Nrf2 is essential for the chemopreventive efficacy of oltipraz against urinary bladder carcinogenesis. Cancer Res. 2004; 64:6424–6431. [PubMed: 15374950]
12. Bieder A, Decouvelaere B, Gaillard C, Depaire H, Heusse D, Ledoux C, Lemar M, Le Roy JP, Raynaud L, Snozzi C, et al. Comparison of the metabolism of oltipraz in the mouse, rat and monkey and in man. Distribution of the metabolites in each species. Arzneimittelforschung. 1983; 33:1289–1297. [PubMed: 6685510]
13. Maxuitenko YY, Libby AH, Joyner HH, Curphey TJ, MacMillan DL, Kensler TW, Roebuck BD. Identification of dithiolethiones with better chemopreventive properties than oltipraz. Carcinogenesis. 1998; 19:1609–1615. [PubMed: 9771932]
14. O'Dwyer PJ, Clayton M, Halbherr T, Myers CB, Yao K. Cellular kinetics of induction by oltipraz and its keto derivative of detoxication enzymes in human colon adenocarcinoma cells. Clin Cancer Res. 1997; 3:783–791. [PubMed: 9815750]
15. Navamal M, McGrath C, Stewart J, Blans P, Villamena F, Zweier J, Fishbein JC. Thiolytic chemistry of alternative precursors to the major metabolite of the cancer chemopreventive oltipraz. J Org Chem. 2002; 67:9406–9413. [PubMed: 12492345]
16. Petzer JP, Navamal M, Johnson JK, Kwak M, Kensler TW, Fishbein JC. Phase 2 enzyme induction by the major metabolite of oltipraz. Chem Res Toxicol. 2003; 16:1463–1469. [PubMed: 14615973]
17. Clapper ML. Chemopreventive activity of oltipraz. Pharmacol Ther. 1998; 78:17–27. [PubMed: 9593327]
18. Levi MS, Borne RF, Williamson JS. A review of cancer chemopreventive agents. Curr Med Chem. 2001; 8:1349–1362. [PubMed: 11562271]
19. Kensler TW, Groopman JD, Sutter TR, Curphey TJ, Roebuck BD. Development of cancer chemopreventive agents: oltipraz as a paradigm. Chem Res Toxicol. 1999; 12:113–126. [PubMed: 10027787]
20. Primiano T, Gastel JA, Kensler TW, Sutter TR. Isolation of cDNAs representing dithiolethione-responsive genes. Carcinogenesis. 1996; 17:2297–2303. [PubMed: 8968041]

21. Egner PA, Kensler TW, Prestera T, Talalay P, Libby AH, Joyner HH, Curphey TJ. Regulation of phase 2 enzyme induction by oltipraz and other dithiolethiones. Carcinogenesis. 1994; 15:177–181. [PubMed: 8313505]

22. Kwak MK, Itoh K, Yamamoto M, Sutter TR, Kensler TW. Role of transcription factor Nrf2 in the induction of hepatic phase 2 and antioxidative enzymes in vivo by the cancer chemoprotective agent, 3H-1, 2-dimethiole-3-thione. Mol Med. 2001; 7:135–145. [PubMed: 11471548]

23. Ramos-Gomez M, Kwak MK, Dolan PM, Itoh K, Yamamoto M, Talalay P, Kensler TW. Sensitivity to carcinogenesis is increased and chemoprotective efficacy of enzyme inducers is lost in nrf2 transcription factor-deficient mice. Proc Natl Acad Sci USA. 2001; 98:3410–3415. [PubMed: 11248092]

24. Lee JS, Surh YJ. Nrf2 as a novel molecular target for chemoprevention. Cancer Lett. 2005; 224:171–184. [PubMed: 15914268]

25. Ko MS, Lee SJ, Kim JW, Lim JW, Kim SG. Differential effects of the oxidized metabolites of oltipraz on the activation of CCAAT/enhancer binding protein-beta and NF-E2-related factor-2 for GSTA2 gene induction. Drug Metab Dispos. 2006; 34:1353–1360. [PubMed: 16714377]

26. Nguyen T, Huang HC, Pickett CB. Transcriptional regulation of the antioxidant response element. Activation by Nrf2 and repression by MafK. J Biol Chem. 2000; 275:15466–15473. [PubMed: 10747902]

27. Dinkova-Kostova AT, Holtzclaw WD, Cole RN, Itoh K, Wakabayashi N, Katoh Y, Yamamoto M, Talalay P. Direct evidence that sulfhydryl groups of Keap1 are the sensors regulating induction of phase 2 enzymes that protect against carcinogens and oxidants. Proc Natl Acad Sci USA. 2002; 99:11908–11913. [PubMed: 12193649]

28. Dinkova-Kostova AT, Massiah MA, Bozak RE, Hicks RJ, Talalay P. Potency of Michael reaction acceptors as inducers of enzymes that protect against carcinogenesis depends on their reactivity with sulfhydryl groups. Proc Natl Acad Sci USA. 2001; 98:3404–9. [PubMed: 11248091]

29. Kim W, Gates KS. Evidence for thiol-dependent production of oxygen radicals by 4-methyl-5-pyrazinyl-3H-1,2-dithiole-3-thione (oltipraz) and 3H-1,2-dithiole-3-thione: possible relevance to the anticarcinogenic properties of 1,2-dithiole-3-thiones. Chem Res Toxicol. 1997; 10:296–301. [PubMed: 9084909]

30. Velayutham M, Villamena FA, Fishbein JC, Zweier JL. Cancer chemopreventive oltipraz generates superoxide anion radical. Arch Biochem Biophys. 2005; 435:83–88. [PubMed: 15680910]

31. Velayutham M, Villamena FA, Navamal M, Fishbein JC, Zweier JL. Glutathione-mediated formation of oxygen free radicals by the major metabolite of oltipraz. Chem Res Toxicol. 2005; 18:970–975. [PubMed: 15962931]

32. Antras-Ferry J, Maheo K, Chevanne M, Dubos MP, Morel F, Guillouzo A, Cillard P, Cillard J. Oltipraz stimulates the transcription of the manganese superoxide dismutase gene in rat hepatocytes. Carcinogenesis. 1997; 18:2113–2117. [PubMed: 9395210]

33. D'Agostini F, Izzotti A, Balansky RM, Bennicelli C, De Flora S. Modulation of apoptosis by cancer chemopreventive agents. Mutat Res. 2005; 591:173–186. [PubMed: 16137721]

34. St-Pierre J, Buckingham JA, Roebuck SJ, Brand MD. Topology of superoxide production from different sites in the mitochondrial electron transport chain. J Biol Chem. 2002; 277:44784–44790. [PubMed: 12237311]

35. Radi R, Turrens JF, Freeman BA. Cytochrome c-catalyzed membrane lipid peroxidation by hydrogen peroxide. Arch Biochem Biophys. 1991; 288:118–125. [PubMed: 1654818]

36. Semak I, Naumova M, Korik E, Terekhovich V, Wortsman J, Slominski A. A novel metabolic pathway of melatonin: oxidation by cytochrome C. Biochemistry. 2005; 44:9300–9307. [PubMed: 15981996]

37. Pereverzev MO, Vygodina TV, Konstantinov AA, Skulachev VP. Cytochrome c, an ideal antioxidant. Biochem Soc Trans. 2003; 31:1312–1315. [PubMed: 14641051]

38. Korshunov SS, Krasnikov BF, Pereverzev MO, Skulachev VP. The antioxidant functions of cytochrome c. FEBS Lett. 1999; 462:192–198. [PubMed: 10580118]

39. Kagan VE, Borisenko GG, Tyurina YY, Tyurin VA, Jiang J, Potapovich AI, Kini V, Amoscato AA, Fujii Y. Oxidative lipidomics of apoptosis: redox catalytic interactions of cytochrome c with

cardiolipin and phosphatidylserine. Free Radic Biol Med. 2004; 37:1963–1985. [PubMed: 15544916]

40. Yang J, Liu X, Bhalla K, Kim CN, Ibrado AM, Cai J, Peng TI, Jones DP, Wang X. Prevention of apoptosis by Bcl-2: release of cytochrome c from mitochondria blocked. Science. 1997; 275:1129–1132. [PubMed: 9027314]
41. Kluck RM, Bossy-Wetzel E, Green DR, Newmeyer DD. The release of cytochrome c from mitochondria: a primary site for Bcl-2 regulation of apoptosis. Science. 1997; 275:1132–1136. [PubMed: 9027315]
42. Butler J, Jayson GG, Swallow AJ. The reaction between the superoxide anion radical and cytochrome c. Biochim Biophys Acta. 1975; 408:215–222. [PubMed: 60]
43. Creutz C, Sutin N. Reduction of ferricytochrome c by dithionite ion: electron transfer by parallel adjacent and remote pathways. Proc Natl Acad Sci USA. 1973; 70:1701–1703. [PubMed: 4352650]
44. Banci L, Bertini I, Liu G, Lu J, Reddig T, Tang W, Wu Y, Yao Y, Zhu D. Effects of extrinsic imidazole ligation on the molecular and electronic structure of cytochrome c. J Biol Inorg Chem. 2001; 6:628–637. [PubMed: 11472026]
45. Lambeth DO, Campbell KL, Zand R, Palmer G. The appearance of transient species of cytochrome c upon rapid oxidation or reduction at alkaline pH. J Biol Chem. 1973; 248:8130–8136. [PubMed: 4356619]
46. Nantes IL, Zucchi MR, Nascimento OR, Faljoni-Alario A. Effect of heme iron valence state on the conformation of cytochrome c and its association with membrane interfaces. A CD and EPR investigation. J Biol Chem. 2001; 276:153–158. [PubMed: 11027687]
47. Salmeen I, Palmer G. Electron paramagnetic resonance of beef-heart ferricytochrome c. J Chem Phys. 1968; 48:2049–2052. [PubMed: 4297179]
48. Everse J, Coates PW. Role of peroxidases in Parkinson disease: a hypothesis. Free Radic Biol Med. 2005; 38:1296–1310. [PubMed: 15855048]
49. Lawrence A, Jones CM, Wardman P, Burkitt MJ. Evidence for the role of a peroxidase compound I-type intermediate in the oxidation of glutathione, NADH, ascorbate, and dichlorofluorescin by cytochrome c/H2O2. Implications for oxidative stress during apoptosis. J Biol Chem. 2003; 278:29410–29419. [PubMed: 12748170]
50. Buettner GR, Jurkiewicz BA. Catalytic metals, ascorbate and free radicals: combinations to avoid. Radiat Res. 1996; 145:532–541. [PubMed: 8619018]
51. Shechter E, Saludjian P. Conformation of ferricytochrome c. IV. Relationship between optical absorption and protein conformation. Biopolymers. 1967; 5:788–790. [PubMed: 6063093]
52. Taylor CP. The EPR of low spin heme complexes. Relation of the t2g hole model to the directional properties of the g tensor, and a new method for calculating the ligand field parameters. Biochim Biophys Acta. 1977; 491:137–148. [PubMed: 191085]
53. Searcy DG, Whitehead JP, Maroney MJ. Interaction of Cu,Zn superoxide dismutase with hydrogen sulfide. Arch Biochem Biophys. 1995; 318:251–263. [PubMed: 7733652]
54. Villamena FA, Zweier JL. Detection of reactive oxygen and nitrogen species by EPR spin trapping. Antioxid Redox Signal. 2004; 6:619–629. [PubMed: 15130289]
55. Muller FL, Liu Y, Van Remmen H. Complex III releases superoxide to both sides of the inner mitochondrial membrane. J Biol Chem. 2004; 279:49064–49073. [PubMed: 15317809]
56. Meany DL, Poe BG, Navratil M, Moraes CT, Arriaga EA. Superoxide released into the mitochondrial matrix. Free Radic Biol Med. 2006; 41:950–959. [PubMed: 16934678]
57. Bielski BHJ, Cabelli DE, Arudi RL, Ross AB. Reactivity of hydroperoxyl/superoxide radicals in aqueous solution. J Phys Chem Ref Data. 1985; 14:1041–1100.
58. Stone JR, Yang S. Hydrogen peroxide: a signaling messenger. Antioxid Redox Signal. 2006; 8:243–270. [PubMed: 16677071]
59. Rhee SG. Cell signaling. H2O2, a necessary evil for cell signaling. Science. 2006; 312:1882–1883. [PubMed: 16809515]
60. Demple B. A bridge to control. Science. 1998; 279:1655–1656. [PubMed: 9518377]

61. Zipper LM, Mulcahy RT. The Keap1 BTB/POZ dimerization function is required to sequester Nrf2 in cytoplasm. J Biol Chem. 2002; 277:36544–36552. [PubMed: 12145307]

62. Huang HC, Nguyen T, Pickett CB. Phosphorylation of Nrf2 at Ser-40 by protein kinase C regulates antioxidant response element-mediated transcription. J Biol Chem. 2002; 277:42769–42774. [PubMed: 12198130]

63. Zipper LM, Mulcahy RT. Inhibition of ERK and p38 MAP kinases inhibits binding of Nrf2 and induction of GCS genes. Biochem Biophys Res Commun. 2000; 278:484–492. [PubMed: 11097862]

64. Kang KW, Lee SJ, Park JW, Kim SG. Phosphatidylinositol 3-kinase regulates nuclear translocation of NF-E2-related factor 2 through actin rearrangement in response to oxidative stress. Mol Pharmacol. 2002; 62:1001–1010. [PubMed: 12391262]

65. Lo SC, Li X, Henzl MT, Beamer LJ, Hannink M. Structure of the Keap1:Nrf2 interface provides mechanistic insight into Nrf2 signaling. EMBO J. 2006; 25:3605–3617. [PubMed: 16888629]

66. Owuor ED, Kong AN. Antioxidants and oxidants regulated signal transduction pathways. Biochem Pharmacol. 2002; 64:765–770. [PubMed: 12213568]

67. Storz P, Doppler H, Toker A. Protein kinase D mediates mitochondrion-to-nucleus signaling and detoxification from mitochondrial reactive oxygen species. Mol Cell Biol. 2005; 25:8520–8530. [PubMed: 16166634]

68. Jemmerson R, Liu J, Hausauer D, Lam KP, Mondino A, Nelson RD. A conformational change in cytochrome c of apoptotic and necrotic cells is detected by monoclonal antibody binding and mimicked by association of the native antigen with synthetic phospholipid vesicles. Biochemistry. 1999; 38:3599–3609. [PubMed: 10090746]

69. Hampton MB, Zhivotovsky B, Slater AF, Burgess DH, Orrenius S. Importance of the redox state of cytochrome c during caspase activation in cytosolic extracts. Biochem J. 1998; 329(Pt 1):95–99. [PubMed: 9405280]

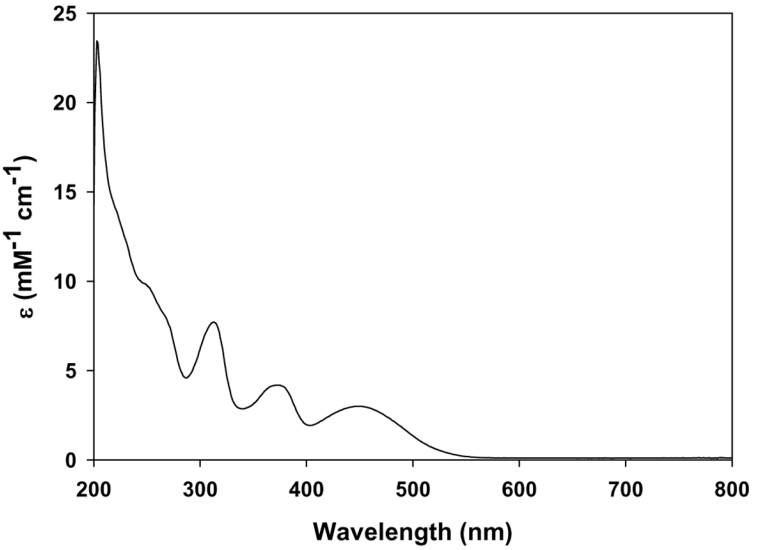

Fig. 1.

UV-visible absorption spectrum of the metabolite PPD formed from the reaction between DTMO (50 μM) and GSH (0.1 mM) in 50 mM phosphate buffer solution (1% acetonitrile), pH 7.4.

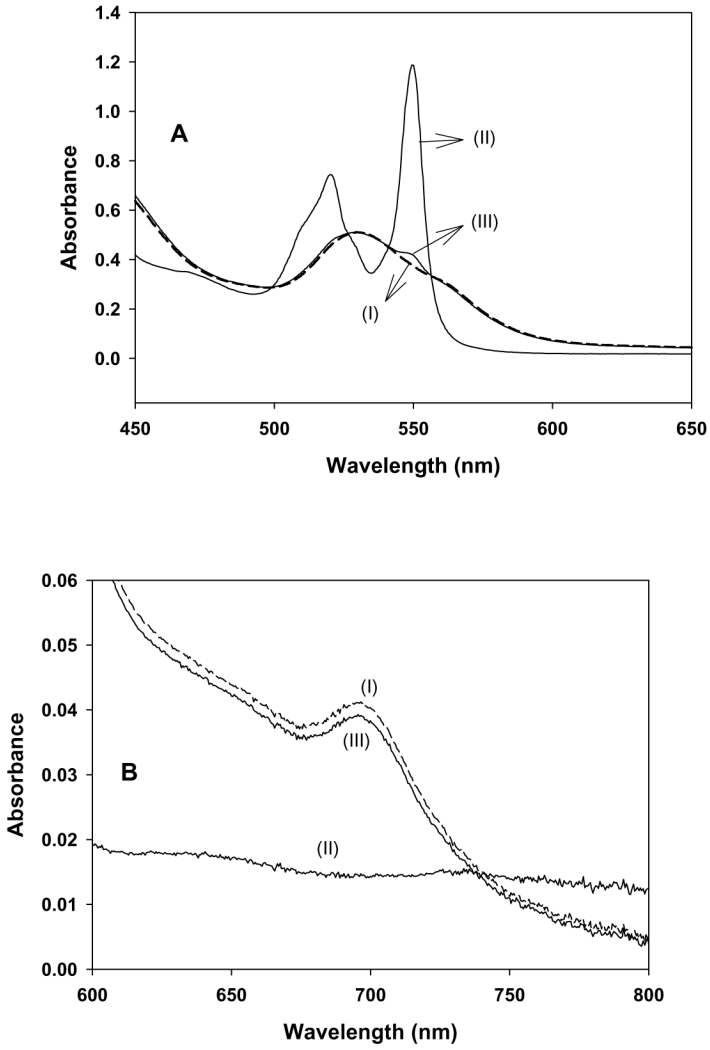

Fig. 2.

UV-visible spectra of oxidized and reduced cytochrome c in phosphate buffer solution (1% acetonitrile) pH 7.4. A: 450 to 650 nm and B: 600 to 800 nm. (I): Fe^{III}cyt c (50 μM). (II): Fe^{III}cyt c (50 μM) and PPD (50 μM). (III):Fe^{III}cyt c (50 μM), PPD (50 μM), and $K_3Fe(CN)_6$ (0.1 mM).

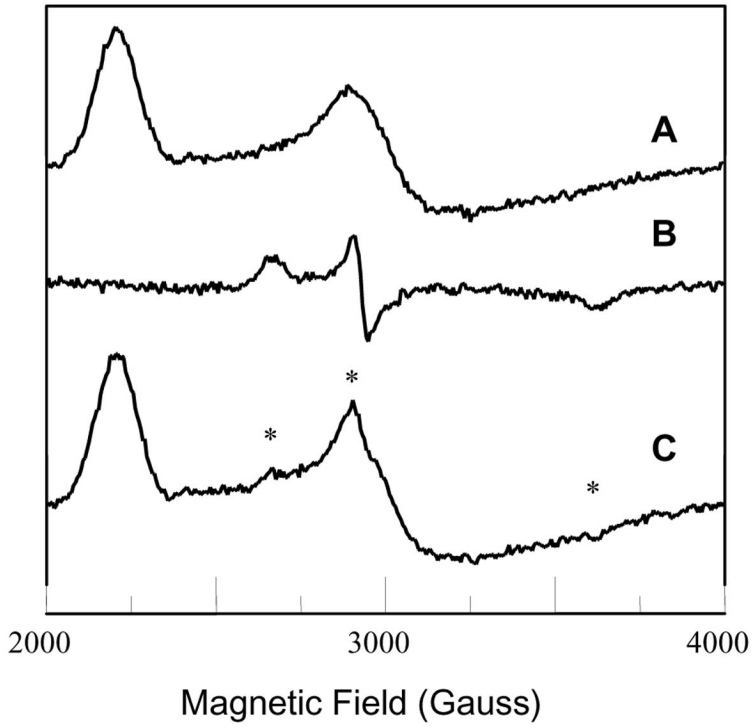

Fig. 3.

Low-temperature (12 K) EPR spectra of oxidized and reduced cyt c. A: Fe^{III}cyt c (0.5 mM); B: Fe^{III}cyt c (0.5 mM) and PPD (0.5 mM), C: Fe^{III}cyt c (0.5 mM), PPD (0.5 mM), and ferricyanide. * - "small populations" of low-spin species from B. The g-values of spectrum A are $g_1 = 3.071$ and $g_2 = 2.234$ (observed) and $g_3 = 1.257$ (calculated). The observed g-values of spectrum B are $g_1 = 2.539$, $g_2 = 2.308$, and $g_3 = 1.87$. EPR instrument parameters used were: modulation amplitude 8 G; time constant 10 ms; sweep time 84 s; microwave power 2 mW; sample temperature 12 K; number of scans 5.

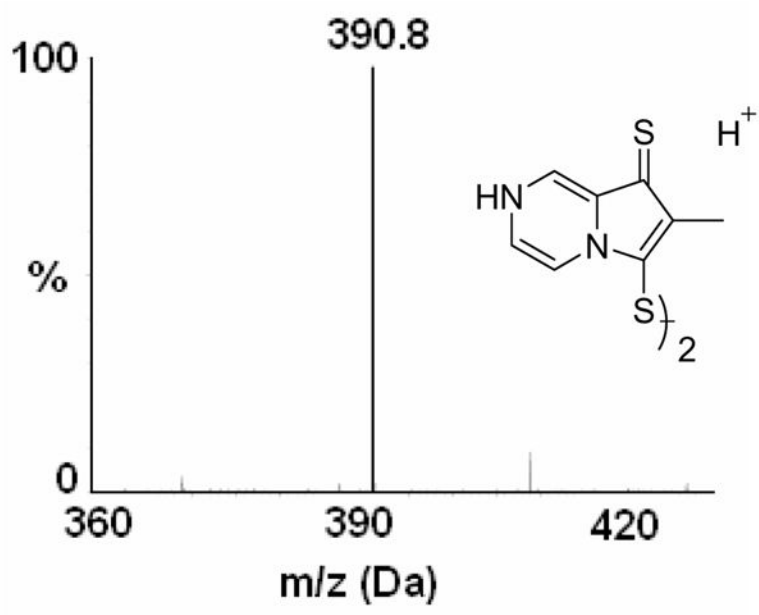

Fig. 4.

ESI-MS analysis (positive ion mode detection) of the reaction product of PPD and cyt c. Mass spectrum corresponds to the dimer of PPD.

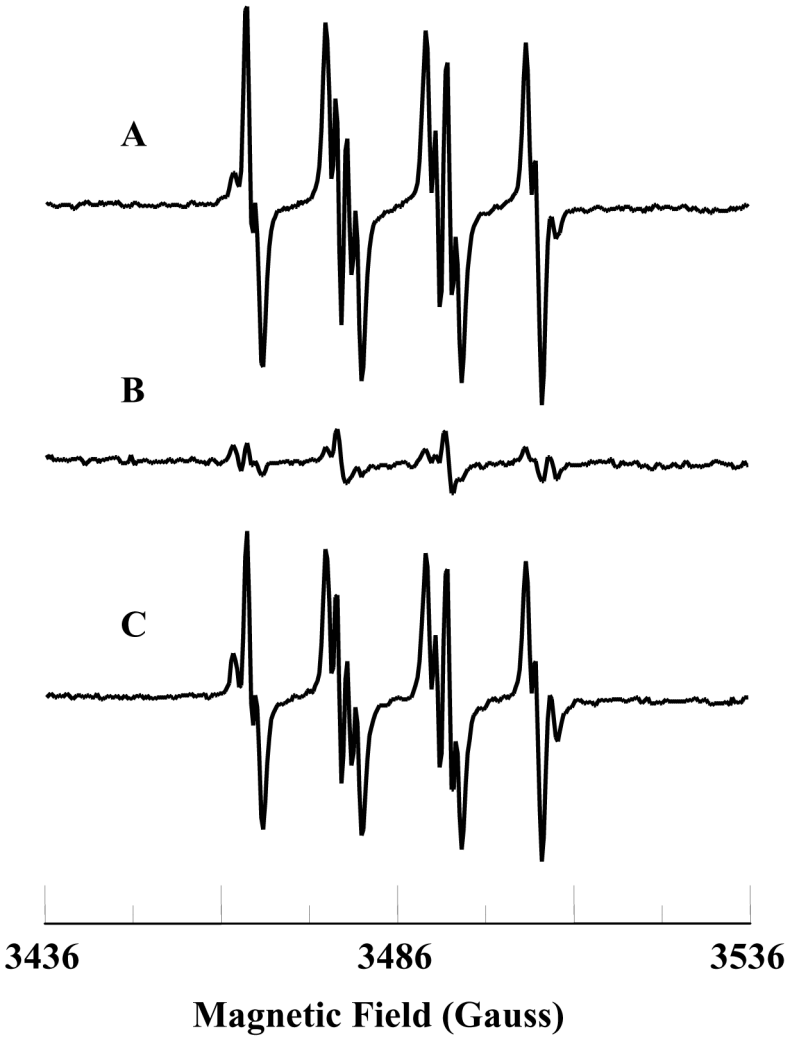

Fig. 5.

EPR spectra of the superoxide radical adduct of DMPO, DMPO-OOH. All the reactions were performed in 50 mM phosphate buffered solution (2 % acetonitrile, pH 7.4). A: DMPO (50 mM), xanthine (333 μM), and XO (0.02 U/mL). B: solution (A) plus Fe^{III}cyt c (0.1 mM). C: solution (A) plus Fe^{III}cyt c (0.1 mM) and PPD (0.1 mM). The observed isotropic hyperfine values of DMPO-OOH adducts are a_N = 14.2 G, a_{H1} = 11.6, and a_{H2} = 1.2 G. EPR instrument parameters used were: microwave frequency 9.775 GHz; modulation frequency 100 kHz; modulation amplitude 0.5 G; microwave power 20 mW; number of scans 10; scan time 30 s; and time constant 82 ms. EPR spectral recording began two minutes after the addition of XO.

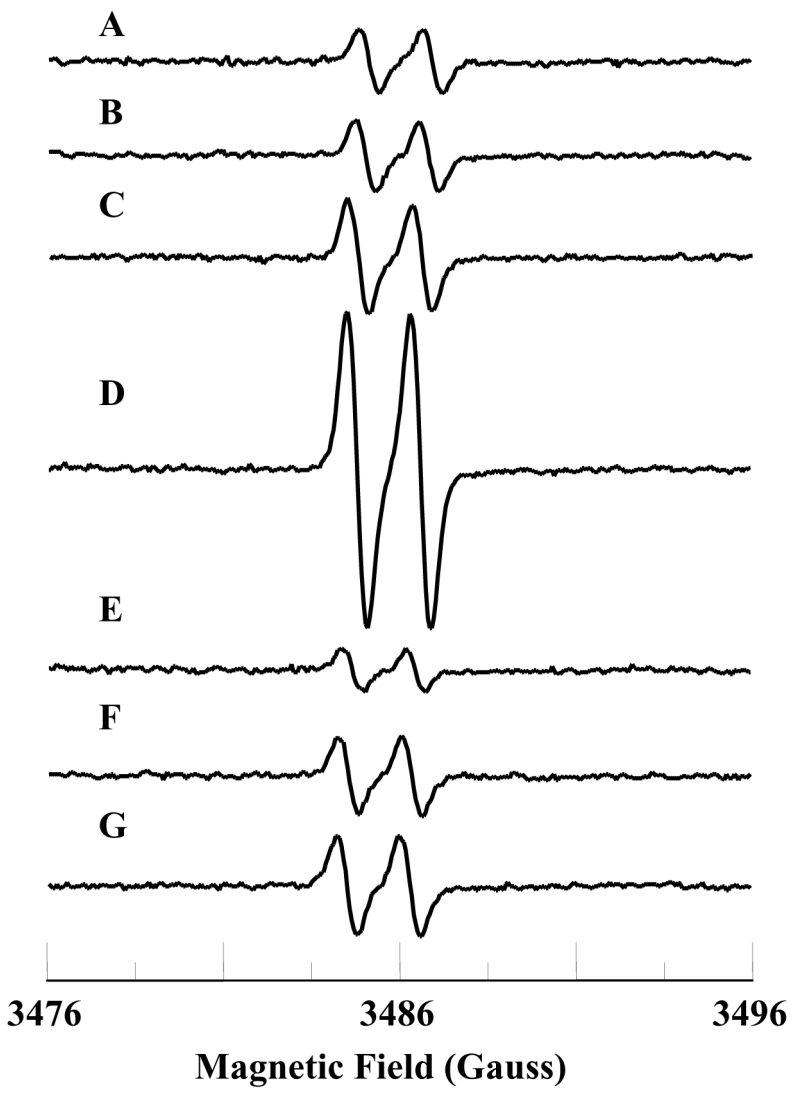

Fig. 6.

EPR spectra of ascorbate radical. The isotropic hyperfine coupling constant of the doublet EPR signal is 1.7 G. A: ascorbate (1 mM); B: ascorbate (1 mM) and hydrogen peroxide (0.25 mM); C: ascorbate (1 mM) and Fe^{III}cyt c (25 μM); D: ascorbate (1 mM), Fe^{III}cyt c (25 μM), and hydrogen peroxide (0.25 mM); E: PPD (25 μM) and ascorbate (1 mM); F: PPD (25 μM), Fe^{III}cyt c (25 μM), and ascorbate (1 mM); G: PPD (25 μM), Fe^{III}cyt c (25 μM), ascorbate (1 mM), and hydrogen peroxide (0.25 mM). All reactions were performed in 50 mM phosphate buffer (pH 7.4). EPR instrument parameters were: microwave frequency 9.775 GHz; modulation frequency 100 kHz; modulation amplitude 0.5 G; microwave power 20 mW; number of scans 10; scan time 30 s and time constant 82 ms. EPR spectra were recorded after 7 minutes.

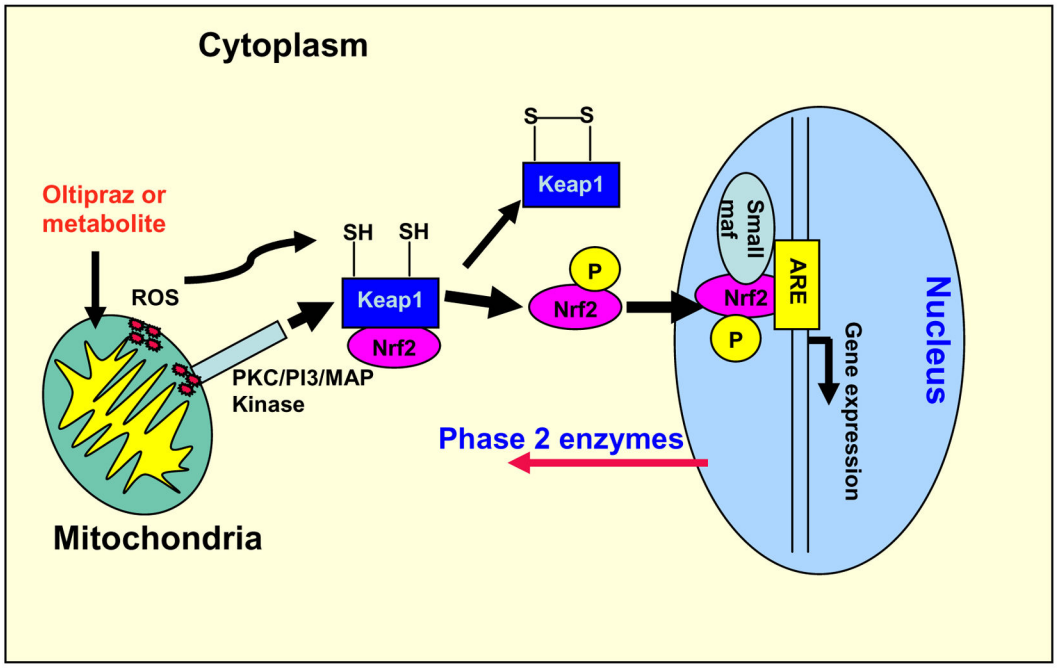

Fig. 7.

Proposed model for the formation of reactive oxygen species at mitochondria, activation of Nrf2, and regulation of phase 2 gene expression in the nucleus.

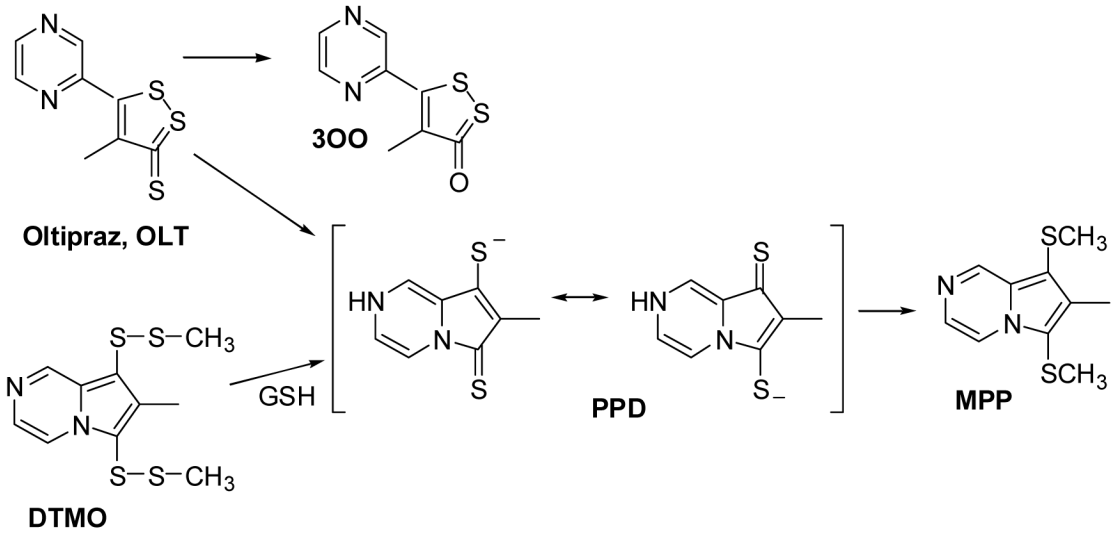

Scheme 1.

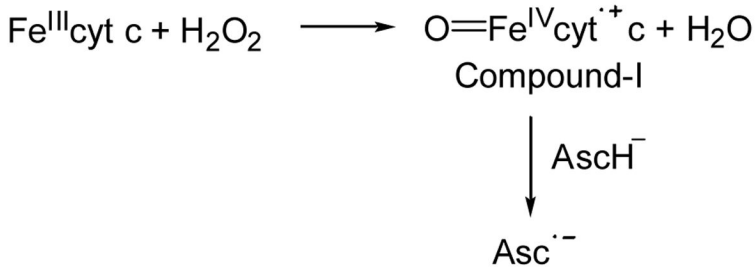

Scheme 2.

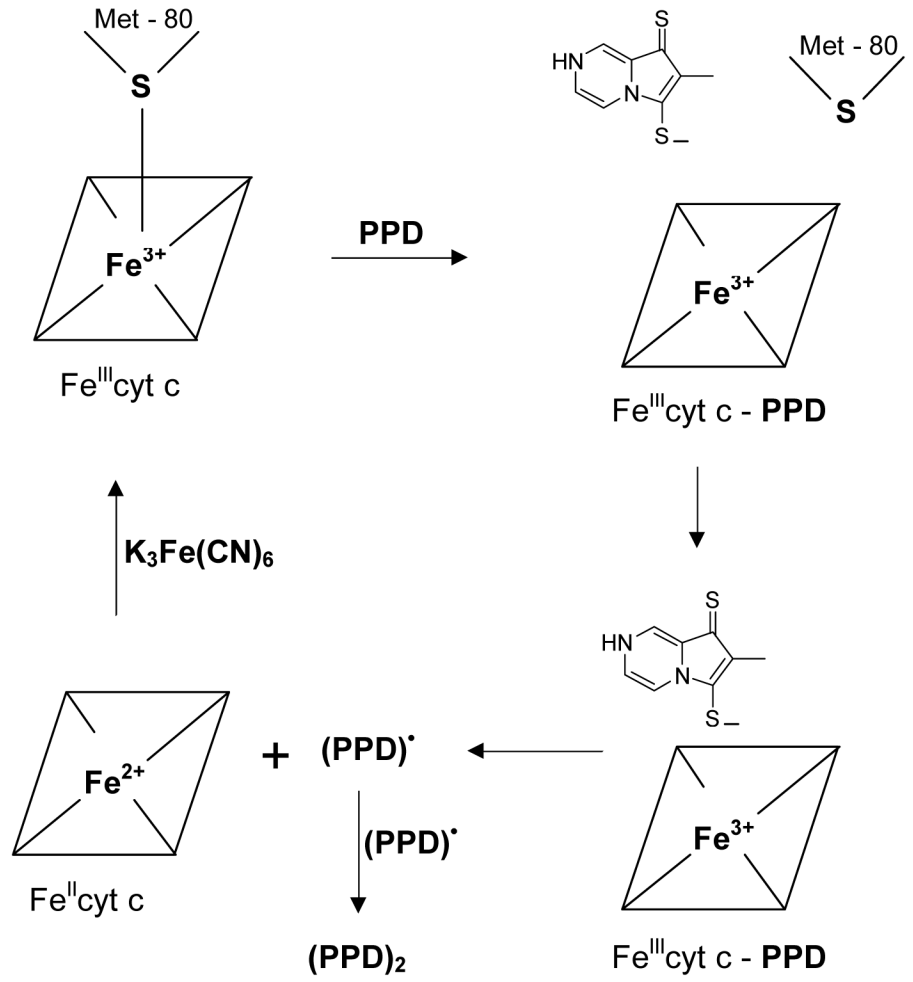

Scheme 3.